Micro-arcsecond light bending by Jupiter

M T Crosta††and F Mignard†

†Observatoire de la Côte d'Azur, UMR CNRS 6202, Le Mont Gros, BP 4229, 06304 Nice cedex 4, France

E-mail: crosta@obs-nice.fr and mignard@obs-nice.fr

Abstract. The detectors designed for Gaia, the next ESA space astrometry mission to be launched in 2011, will allow to observe repeatedly stars very close to Jupiter's limb. This will open a unique opportunity to test General Relativity by performing many Eddington-like experiments through the comparison between the pattern of a starfield observed with or without Jupiter. We have derived the main formulas relevant for the monopole and quadrupole light deflection by an oblate planet and developed a simulator to investigate the processing of the Gaia astrometric observation in the vicinity of the planet. The results show that such an experiment carried out with the Gaia data will provide a new fully independent determination of γ by means of differential astrometric measurements and, more importantly, for the first time will evidence the bending effect due to the quadrupole moment with a 3σ confidence level. Given the accuracy of the experiment for the monopole deflection, this will permit to test alternative modelling of the light bending by moving masses.

Submitted to: *Class. Quantum Grav.*

† Present address: Observatory of Turin, Strada Osservatorio 20, Pino Torinese (To), Italy

1. Introduction

Several key questions of modern astrophysics regarding the formation and evolution of the Milky Way will be clarified with the next space astrometry mission Gaia, approved in 2000 as a cornerstone within the European Space Agency science program [1]. The mission is now funded and will enter in the C/D phase in 2006 for a launch scheduled in late-2011 and nominal operations over the next five years. Thanks to its high precision (10 μarcsecond in angular measurements) and multi-epoch astrometry, Gaia will be able to detect the relative positional change of a star resulting for the tiny curvature of the light ray brought about by the gravitational pull of the Sun, and to a lesser extent by the giant planets.

As far as the light deflection produced by the solar mass is concerned, the science case has included from the outset an investigation of the value of the PPN parameter γ, considered as a global unknown in the astrometric model. This parameter, equal to one in General Relativity (GR), indicates the amount of space-time curvature produced by a unit rest-mass and it is a fundamental part of the so called parameterized Post-Newtonian (PPN) formalism [2], originally developed by Eddington for the famous experiment during the solar eclipse in 1919. The PPN method aims to quantify the violations of the Equivalence Principle by parameterizing deviations which modify both local physical laws and large-scale gravitational phenomena, including the constancy of the constants. PPN formalism is valid for a broad class of metric theories and includes GR as a reference case, *i.e.* as a current standard theory of gravitation. The slow motion and weak field limit allows to use PPN metric expansion as a function of several parameters, varying from theory to theory, useful to discern gravitational experiments in the Solar System. The PPN parameter γ is the most important, since all the other parameters to all relativistic order within the alternative theories to gravity, converge to their GR value in proportion to $|1-\gamma|$ [3].

The most general formulation of these theories contains an arbitrary function of a scalar field coupled to the stress-energy tensor in order to merge quantum mechanics with gravity. Recent works on scalar-tensorial theories consistent with various cosmological scenarios suggest the search for discrepancies from unity of γ at the levels of 10^{-5} to 10^{-7}; more precisely, Damour and Nordtvedt [4] assume that there exist a cosmological attractor mechanism towards GR quantified from deviation of γ from unity within the above level of accuracy depending on the total mass density of the Universe. Then, an experiment purposely designed could reveal the coexistence of the two mentioned fields throughout the cosmological evolution up to the present where pure tensor gravity explains the gravitational interaction from small to large scale. In addition, some dynamical models predict scalar fields dominating the current energy density of the universe, which should contribute to the value of γ at the level of 10^{-7} to 10^{-9}, thus providing a universe evolution without the need of dark matter [3]. All this issues make precision tests of gravity in space a fascinating challenge for the next decades, as in the past the Eddington's observations in 1919 of star line-of-sight did, confirming the

amount of $1\farcs72$ as deflection angle predicted by GR. Nowadays, all present experimental tests are compatible with the predictions of GR. In particular, experiments conducted in Solar System have tested all the weak-field predictions of GR theory at better than the 10^{-3} level and down to 2×10^{-5} level for γ as seen from the additional Doppler shift in radio-wave beams connecting the Earth to the Cassini spacecraft when they passed near the Sun [5].

New space projects will go deeper in experimental gravitation. The NASA Gravity Probe B mission [6], whose first results are expected very soon, should directly measure γ to better than the 10^{-5} level, although this is not the main objective of the experiment and remains subjected to efficient instrumental calibrations. An early analysis of the Gaia's capabilities, indicates that its measurements should provide a precision of 5×10^{-7} for this parameter [7, 8], an improvement of more than two orders of magnitude to the current best estimate mentioned above. This is quite comparable to the expectations of the LATOR project [9], which is designed to use two optical interferometers between two micro-spacecrafts and aims to determine $|1-\gamma|$ at the level of 10^{-8}.

Besides the determination of γ based on the global astrometry capabilities of Gaia, the mission will also allow to carry out dedicated small field experiments from the observations performed close to the surface of a giant planet like Jupiter or Saturn. The light bending due to their gravitational field will be detectable in the visible and we show in this paper that even the quadrupole field of Jupiter will be evidenced in such an experiment. It is therefore possible to carry out the same kind of eclipse experiment made by Dyson, Eddington, and Davidson in 1920, but now by comparing stellar positions in the immediate vicinity of the planets. Not only will this experiment be a further confirmation of a GR prediction, but it will also help understand the very difficult question of the light-bending by a moving source and that of the propagation of gravitation.

Using Jupiter to test GR, Kopeikin and Fomalont claimed they have determined the speed of gravity trough the VLBI ‡ astrometric measurement of Shapiro time delay of light from the Quasar J0842+1835, as its image passed within 3.7 arcmin of the planet (about 10 Jupiter radii, a far cry from what Gaia can achieve) [10]. According to the post-Minkowskian formalism assumed [11], the gravitational field due to a moving body propagates with finite speed; consequently, it influences a photon with some retardation. The speed of gravity enters as an extra tiny velocity-dependent corrections to the Shapiro time delay formula of the order of 4.8 ps. At present there is no general consensus on the results, especially upon the method to extend GR to the case where the velocity of gravity differs from the velocity of light [12, 13]. In particular, given the observed limits on γ, the Fomalont-Kopeikin measurements are not accurate enough yet to determine the speed of gravity [12]. Some authors interpret the result within the Lorentz transformation properties of the weak gravitational field and consider it as a violation not only of the Lorentz invariance but also of the Galilean one [14,15]. Paper [16] settles

‡ VLBI is the acronym for Very Long Baseline Interferometry

	$\delta\Phi_{\rm pN}$	$\delta\Phi_Q$	$\delta\Phi_{\rm max}$
Sun	$1''.75$	~ 1 μas	(180°)
	μas	μas	
Mercury	83	–	$9'$
Venus	493	–	4.5°
Earth	574	0.6	178°
Moon	26	–	9°
Mars	116	0.2	$25'$
Jupiter	16280	239	$90^\circ/3'$
Saturn	5772	94	$18^\circ/51''$
Uranus	2081	25	$72'/6''$
Neptune	2535	9	$51'/3''$
Pluto	7	–	$8''$

Table 1. Light deflection amounts at 1 μarcsec due to the planets for a photon crossing the Solar System: pN is for post-Newtonian order and Q for the quadrupolar moment. The values are computed for grazing rays in the Gaia observing geometry; figures in the last column give the angular distances between the perturbing body and the star at which the effect is still 1 μarcsecond, with Gaia at the Sun-Earth L2. Where two values are reported they refer, respectively, to pN and quadrupole effect.

the significance of the Jupiter experiment as a simply standard aberration of light which propagates across an active medium with an effective index of refraction induced by the gravitational field of a lens in motion: the tiny corrections to the Shapiro time delay should be included into the fitting of microlensing events. However, even if there is still a controversy about the question of whether the results depend on the speed of gravity [17] or on the abberation of light [14, 16, 18], there is a general agreement that this measurement is a remarkable precise VLBI detection of a post-Newtonian effect due to a planet.

The possibility to apply methods of relativistic astrometry to test GR has prompted several groups to model highly accurate angular observations in the relativistic framework. New formalisms have been proposed ([11, 19–21] and reference therein) to tackle the relativistic problem of the light path reconstruction, which, at least at the μas accuracy, implies taking into account all the contributions not only due to the bulk mass of the Solar System bodies, but also to their quadrupole moment and to the time-dependent gravitational field generated by their motions (see table 1).

In particular, two papers [22] and [23] have gone through the post-Newtonian treatment of the light propagation in the case of an isolated axisymmetric body, in order to take into account the influence of the multipole moments. The former is based

on a mathematical solution of geodesic equation whereby mathematical expressions for the light deflection in any order of multipole perturbations are obtained. In the second paper, this contribution stems from the prior computation of the time transfer function between two point located at a finite distance. However neither approach has provided hints on how to apply the intricate formulas to a practical case like the one faced in the Gaia modelling.

Having in mind the capabilities of Gaia to observe stellar sources very close to Jupiter's limb (at a fraction of the planet radius), we have evaluated the light deflection produced by an oblate planet on grazing photons coming from distant stars. This study is part of a wider project called GAia Relativistic EXperiment (GAREX), which aims to investigate all possibilities to test GR with Gaia measurements. In the solar system, this mission will mainly carry out:

- light deflection experiments, divided into (i) global astrometry, in particular highly accurate determinations of γ by observing the change in star position at different angular distance to the Sun; (ii) small field experiments, with the examination of the light propagation by means of differential measurements of stellar positions near the planets;
- perihelion precession effect, related to the determinations of PPN parameter β § from the orbit fitting of several thousands minor bodies [24].

In this paper we concentrate on the case of the light bending by Jupiter at the microarcsecond level and its detection by the small field astrometric observations with Gaia. In [25] we have already explored the favorable circumstances for Gaia in five years of continuous observations, approximately from 2012 to 2017, to detect the quadrupole light bending effect predicted by GR, but never observed. For Jupiter the magnitude of the monopole deflection for a grazing ray is ~ 16 milliarcsecond, to which a component from the quadrupole moment is superimposed with an amplitude of $\sim$ 240 microarcsecond, as showed in table 1. This secondary deflection has a very specific pattern as a function of (i) the position of the star with respect to the oblate deflector and (ii) the orientation of its spin axis. In section 2 we derive the relevant formulas to express this light bending effect using the PPN formalism at large and small angle from the planet. In section 3 we describe all the steps needed to simulate the small field experiment when observing stellar background in vicinity of Jupiter. Finally, in section 4, we discuss the data processing of a set of Montecarlo runs and the results in the determination of the PPN Parameter γ and the quadrupole effect from Jupiter.

2. The light deflection produced by an axisymmetric planet

Most stellar sources, planets and observers have a small velocity compared to the velocity of the light and a weak inter-body gravitational field exists inside bound systems. Moreover, if we consider isolated distribution of matter, the geometry can

§ The PPN parameter β measures the non-linearity in the superposition of gravitational fields.

be assumed Minkowskian, asymptotically flat far away [26]. Let us consider, then, a set of PPN coordinates $\{x^\alpha\}$ ($\alpha = 0, 1, 2, 3$) and a solar system locally perturbed by isolated stationary axisymmetric masses. To the post-Newtonian (pN) accuracy, the spatial part of the geodesic equation of a light ray coming form a distant star can be easily transformed into [2]:

$$\frac{d^2x^i}{dx^{0\,2}} = U_{,i}\left(1+\gamma\,\delta_{jk}\frac{dx^j}{dx^0}\frac{dx^k}{dx^0}\right) - 2(1+\gamma)\frac{dx^i}{dx^0}\left(\delta_{jk}\frac{dx^j}{dx^0}U_{,k}\right), \tag{1}$$

where $U = M/\sqrt{(\delta_{ij}x^ix^j)}$ ($i, j, k = 1, 2, 3$) is the Newtonian potential (in geometrized units) and $U_{,i}$ its partial derivative with respect to the spatial coordinates. A solution of the above equation can be get by tracing a Newtonian zero order straight-line x^i_N plus all the relativistic deviations x^i_D, *i.e.*

$$x^i = x^i_N + x^i_D. \tag{2}$$

Then, by decomposing x^i_D into two components, parallel ($x^i_{D_\parallel}$) and perpendicular ($x^i_{D\perp}$) to x^i_N, equation (1) becomes

$$\frac{d^2x^i_{D\perp}}{dx^{0\,2}} = (1+\gamma)[U_{,i} - t^i(\delta_{jk}t^jU_{,k})] = (1+\gamma)\nabla_\perp U, \tag{3}$$

where $\mathbf{t} = dx^i/dl$ is the unit tangent vector on the unperturbed light path in the direction of the observer. Here the symbol $\nabla_\perp$ indicates the derivative perpendicular to the light ray, assumed to pass outside the matter distribution. Placing the origin of coordinates x^i_0 at the center of an axisymmetric planet, *i.e.* $\mathbf{z}$ considered as its axis of maximum moment of inertia, located between the star and the observer, the positional vector of the photon with respect to the principal axes centered at the planet can be expressed as:

$$r^i = x^i - x^i_0 = t^i\ell - n^ib, \tag{4}$$

where ℓ represents the length of the light path and $\mathbf{n}$ the radial direction perpendicular to the unperturbed ray pointing towards the center of gravity, along the impact parameter b.

The light deflection is given by the deviation of the tangent vector $\mathbf{t}$ from the straight-line along the photon's path as,

$$\Delta\mathbf{\Phi} \equiv \int \frac{d\mathbf{t}}{d\ell}d\ell \tag{5}$$

which leads with (3) to,

$$\Delta\mathbf{\Phi} = (1+\gamma)\int \nabla_\perp U\, dl. \tag{6}$$

By taking the gravitational potential up to the quadrupole term one gets,

$$\begin{aligned}\nabla_\perp U = &\left[-\frac{b}{r}\left(-\frac{M}{r^2} + \frac{3M}{r^4}J_2R^2\frac{5\cos^2\theta - 1}{2}\right)\right.\\ &\left. + \left(-\frac{3M}{r^4}J_2R^2\cos\theta\right)(\mathbf{z}\cdot\mathbf{n})\right]\mathbf{n}\\ &+ \left(-\frac{3M}{r^4}J_2R^2\cos\theta\right)(\mathbf{z}\cdot\mathbf{m})\mathbf{m}\end{aligned} \tag{7}$$

where r and θ are respectively the radial distance and the co-latitude (measured from the planet north pole) of a field point on the light trajectory, J_2 is the dimensionless coefficient of the second zonal harmonic, R the radius and M the mass of the planet, and, finally, **m** represents the orthoradial component (see figure 1 and figure 2).

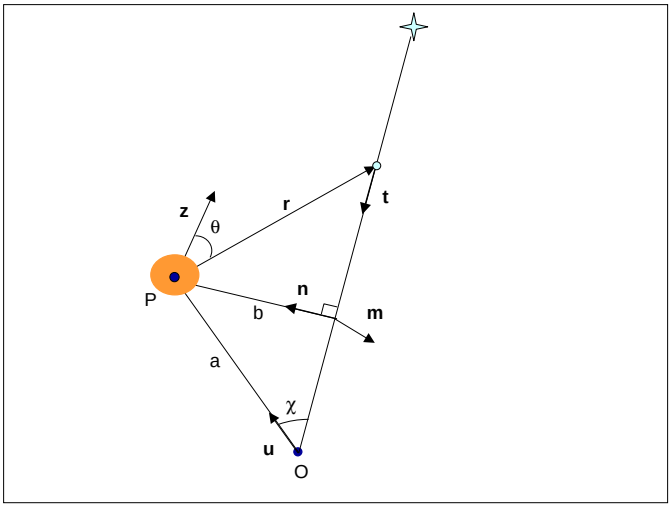

Figure 1. Geometry of light deflection due to a planet (P): the spin axis of the planet **z** is out of the plane; **t** represents the unit tangent vector from a distant star (S) to the observer (O) on the unperturbed light trajectory; **u** is the unit direction from O to P along their distance a; finally, χ is the angle $S\hat{O}P$, and b the impact parameter.

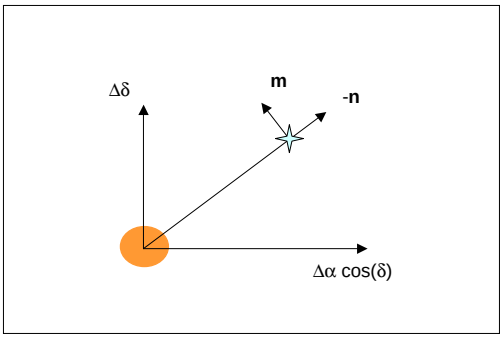

Figure 2. Light deflection by a planet: tangent plane on the sky. The position of the star is displaced both in the radial (**-n**) and orthoradial **m** directions. The spin axis of the planet **z** (not shown here) does not lie in this plane in general.

The length ℓ of the photon path can be scaled by the impact parameter into a dimensionless parameter as follows

$$d\ell = bd\lambda, \tag{8}$$

so the radial distance becomes

$$r = b(1+\lambda^2)^{1/2}. \tag{9}$$

Each integral entering (6) must be computed with λ running positively in the same direction as the photon from $\lambda = -\infty$ to $\lambda = 1/\tan\chi$, with χ standing for the angular separation between the directions star/observer and observer/planet (figure 1). At the closest approach on the unperturbed ray one has $\lambda = 0$. The explicit expressions of the integrals are given in appendix A. After some algebra, the light deflection vector is split into two components, the first one along $\mathbf{n}$ and the second one along $\mathbf{m}$, both including the monopole and the quadrupole contribution of the planet in function of the angular separation χ:

$$\Delta\mathbf{\Phi} = \Delta\Phi_1\mathbf{n} + \Delta\Phi_2\mathbf{m}, \tag{10}$$

where, precisely,

$$\begin{aligned}\Delta\Phi_1 = (1+\gamma)\frac{2M}{b}\Bigg\{&(1+\cos\chi) + J_2\frac{R^2}{b^2}\Big[(1+\cos\chi+\frac{1}{2}\cos\chi\sin^2\chi)\\ &-2(1+\cos\chi+\frac{1}{2}\cos\chi\sin^2\chi+\frac{3}{4}\cos\chi\sin^4\chi)(\mathbf{n}\cdot\mathbf{z})^2\\ &+(\sin^3\chi-3\sin^5\chi)(\mathbf{n}\cdot\mathbf{z})(\mathbf{t}\cdot\mathbf{z})\\ &-\ (1+\cos\chi+\frac{1}{2}\cos\chi\sin^2\chi-\frac{3}{2}\cos\chi\sin^4\chi)(\mathbf{t}\cdot\mathbf{z})^2\Big]\Bigg\}\end{aligned} \tag{11}$$

and

$$\begin{aligned}\Delta\Phi_2 = \frac{(1+\gamma)MJ_2R^2}{b^3}\Big[&2(1+\cos\chi+\frac{1}{2}\cos\chi\sin^2\chi)(\mathbf{n}\cdot\mathbf{z})(\mathbf{m}\cdot\mathbf{z})\\ &+\sin^3\chi(\mathbf{m}\cdot\mathbf{z})(\mathbf{t}\cdot\mathbf{z})\Big].\end{aligned} \tag{12}$$

The first term in the radial component (that along $\mathbf{n}$) is the classical monopole deflection, widely used in astronomy. All the other terms factored by J_2 come from the quadrupole of the planet. One can specialize these expressions to near-grazing rays as, unlike with the solar deflection, the effect is too small to be observed at large angle from the planet. Hence when $\chi \ll 1$ this leads to the more convenient and accurate enough formulas,

$$\Delta\Phi_1 = \frac{2(1+\gamma)M}{b}\left[1 + J_2\frac{R^2}{b^2}\left(1-2(\mathbf{n}\cdot\mathbf{z})^2-(\mathbf{t}\cdot\mathbf{z})^2\right)\right] \tag{13}$$

$$\Delta\Phi_2 = \frac{4(1+\gamma)MJ_2R^2}{b^3}(\mathbf{m}\cdot\mathbf{z})(\mathbf{n}\cdot\mathbf{z}). \tag{14}$$

which are similar to a derivation obtained in [27] in the case of the Sun.

The deflection vector depends on the orientation of the spin axis of the planet and, moreover, on the direction of the star with respect to the planet as seen in the terms proportional to $(\mathbf{n}\cdot\mathbf{z})$ and $(\mathbf{t}\cdot\mathbf{z})$. In general the quadrupole deflection vector depends both on the impact parameter and on the direction of the light source with respect to the spin axis projected on the plane of the sky. However, for a given impact parameter, its modulus (10) depends only on the star's direction with respect to the planet's reference

frame. This property is established in Appendix B and has been used thoroughly to as an additional check to the computer implementation of the simulation (see section 3.2). One should note that the above formulation has left aside and neglected refinements in the modelling like the motion of Jupiter, the retarded effect on the light propagation and mulipolar terms of higher orders in the potential expansion.

Considering $\gamma = 1$ is equivalent to saying that equations (13)-(14) constitute the reference modelling in the standard GR. Therefore, in the same way as one introduces γ in the monopole deflection to characterize departures from GR, we multiply J_2 by a dimensionless parameter ϵ whose value is 0 if no effect is seen (say this may correspond to a lack of coupling between gravity and electromagnetism seen in the multipole moments) and 1 for the standard GR. Hereafter we call this parameter the Quadrupole Efficiency Factor (QEF) and the goal is to see whether it is significantly determined from the Gaia observations. Although ϵ is not a PPN parameters, it represents the first level of a post-Newtonian test whose goal is to determine whether the effect is detected,*i.e.* if one can say that ϵ is equal to unity, with a certain uncertainty. Thus, for the processing of the experiment of light deflection near the planet, we adopt the following formulation,

$$\Delta\Phi_1 = \frac{2(1+\gamma)M}{b}\left[1 + \epsilon J_2 \frac{R^2}{b^2}\left(1 - 2(\mathbf{n}\cdot\mathbf{z})^2 - (\mathbf{t}\cdot\mathbf{z})^2\right)\right] \tag{15}$$

$$\Delta\Phi_2 = \frac{4M(1+\gamma)\epsilon J_2 R^2 \gamma}{b^3}(\mathbf{m}\cdot\mathbf{z})(\mathbf{n}\cdot\mathbf{z}). \tag{16}$$

including the two unknowns γ and ϵ, which are equal to 1 in the simulation.

3. Small field experiments with Jupiter

The one GAREX experiment we consider in this paper is a light deflection in the vicinity of Jupiter. The goal is to measure in a fully independent way the two parameters γ and ϵ expressed in light deflection formulae (15) and (16), together with their associated errors, knowing the astrometric accuracy that will be achieved by Gaia. As J_2 is well known from space probe tracking with a precision better than 10^{-5}, we will here consider it as a constant, and infer instead an estimate of the QEF factor ϵ.

3.1. Ephemerides

First, we have investigated what are the favorable circumstances to perform experiments using Jupiter during the mission lifetime [25]. This depends on the number of times Jupiter will cross one of the astrometric fields during the mission and on the stellar density in its immediate surroundings during these observations. At present, the details of the former can only be known statistically, as the precise initial conditions of the sky scanning law remain unknown. On the other hand the sky background can be assessed with more certainty as it depends only on the motion of Jupiter between 2012 and 2018, and not very accurately on when the observations take place, provided they are reasonably scattered during the observing period. The ephemerides of Jupiter have been

computed in galactic coordinates between these two epochs for an observer orbiting the Sun-Earth L2 in the same way as Gaia will do. The observability conditions are shown in figure 3 with the visibility periods when the angular distance to the Sun makes the observations feasible with Gaia (no observations can be made around conjunctions and oppositions). Galactic coordinates are used just because the primary dependence of the stellar density is on the galactic latitude.

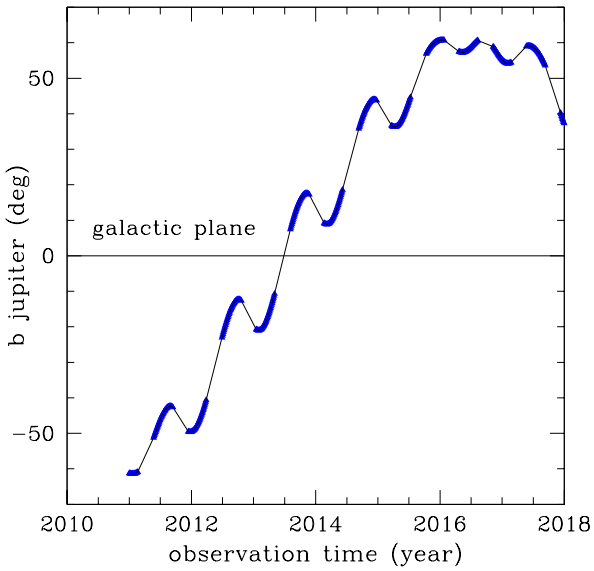

Figure 3. Galactic latitude (b) of Jupiter versus the observing time (in years). The solid line represents the galactic latitude of Jupiter (as seen from Gaia) over the years 2011-2018 and the highlighted patches correspond to the visibility periods when the angular distance to the Sun makes the observation possible.

We have chosen the date 2012 as the beginning of the simulations, since Gaia will take at least six months to be operational at the Lagrangian point L2 of the Earth-Moon-Sun system. Jupiter will cross the galactic plane in mid-2013 and, consequently, we expect favorable observations of the planet in front of a dense stellar background as shown in figure 4. The plot gives the average number of stars per square degree around Jupiter from 2012 to 2018 as seen from Gaia.

3.2. Simulation of the experiment

The principle of the simulated experiment is to generate a series of pairs of observations over the mission length of 5 years, so that in each pair Jupiter is, or is not, at the center of the stellar field. In both cases astrometric observations similar to that expected from Gaia are computer generated, with the proper noise function of the star brightness. The number of stars simulated in each field is determined by the galactic latitude of Jupiter at the observation time. Then the two star patterns are compared and the differences in along-scan positions (the only direction of accurate measurements with Gaia) are fitted

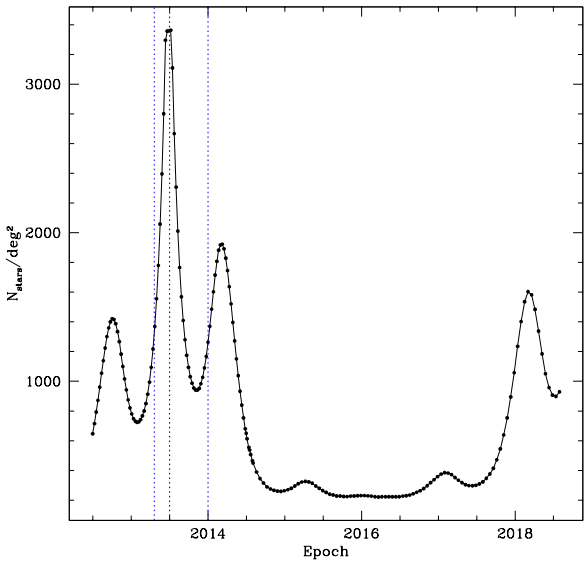

Figure 4. Mean number of stars per square degree down to the magnitude limit V=20 in the field of Jupiter during the Gaia operations. The dashed lines represent the period when Jupiter crosses the galactic plane and the central one the epoch when the maximum number of stars is observed.

to the model with the two unknowns γ and ϵ. This is an idealized version of the Gaia procedure as the two fields (with or without Jupiter) will not be observed exactly a the same time, leading to correction for the relative orientations of the fields and for the proper motion of the stars. But these are technical details that will be carefully handled during the data processing and have no impact on the feasibility study demonstrated in this paper. The numerical parameters used in the simulation are listed in table 2.

In order to use equations (15)-(16) in the simulation, we have fixed the origin of the coordinate system at Jupiter's center and assumed that it coincides with the center of the astrometric focal plane. Given the galactic coordinates (l, b) of Jupiter we extracted the relevant stellar density in the magnitude range $V = 12.0 - 20.0$ from a realistic galactic model based in actual star counts fitted to convenient mathematical expressions as a function of the galactic latitude and longitude. The magnitude range is determined by the rejection of saturated stars (brighter than V=12.0) on the bright side and by keeping stars observable with Gaia with a reasonable astrometric accuracy on the faint side. One must keep in mind that the number of close approaches between Jupiter and stars brighter than $V \simeq 12$ will be a rare event, albeit very important in this context, but not liable to statistical treatment. It must be handled on a case by case basis with a real sky and this will be done later when the final parameters of the scanning law are known. After having computed the number of stars per interval of 0.5 magnitude inside the field of view at each observational epoch, we generated the observed stars in the field of view. For the fields with Jupiter we have computed the

Table 2. Main parameters used for the simulation.

parameter	numerical value
number of observations	90
area of the field-of-view	0.6 deg × 0.6 deg
magnitude range	12.0 to 20.0
R_J	7.13×10^7 m
$M = GM_J/c^2$	1.41 m
Jupiter J_2	0.014736
γ	1
ϵ	1
$\sigma_{\rm pos}$ along the scan at $V = 15$	100μas
$\sigma_{\rm pos}$ across the scan at $V = 15$	300μas

proper stellar directions by taking into account the full deflection due to the monopole and the quadrupole. Then for any pair and any epoch we have added a gaussian noise in both coordinates. The standard deviation of the noise is determined by the magnitude of the star and the coordinates (along- or across-scan) with [1]:

$$\sigma_{als} = a \times 10^{0.2(V-15)} \tag{17}$$

for stars with magnitude $V > 12.5$. The coefficient a is the scaling factor giving the single observation astrometric accuracy for a star of 15 magnitude. For stars brighter than 12.5, σ_{als} is constant and chosen to be 30 μas for the measurements along the scan and 100 μas across. We have used the property expressed in (B.3) to cross-check the contribution of the quadrupole term in the simulation. Other checks were also performed in different reference frames that helped improve the reliability of the simulator. Figure 5 and figure 6 illustrate several important features of the simulated data.

The plots in figure 5 show the absolute values of the monopole and of the quadrupole deflections, obtained with the simulator for the different epochs and impact parameters. Figure 6 is an example of the observed field corresponding to mid 2013 when Jupiter crosses the Galactic plane. Even if this date represents a favorable observation, the relatively limited number of stars close to Jupiter does not lead to an obvious signature of the stellar displacements produced, in particular, by the quadrupole effect. For this reason we have also plotted the cumulative effect in figure 7 by combining all the epochs. As expected one sees clearly the radial nature of the monopole deflection and the more complex pattern of the quadrupole effect.

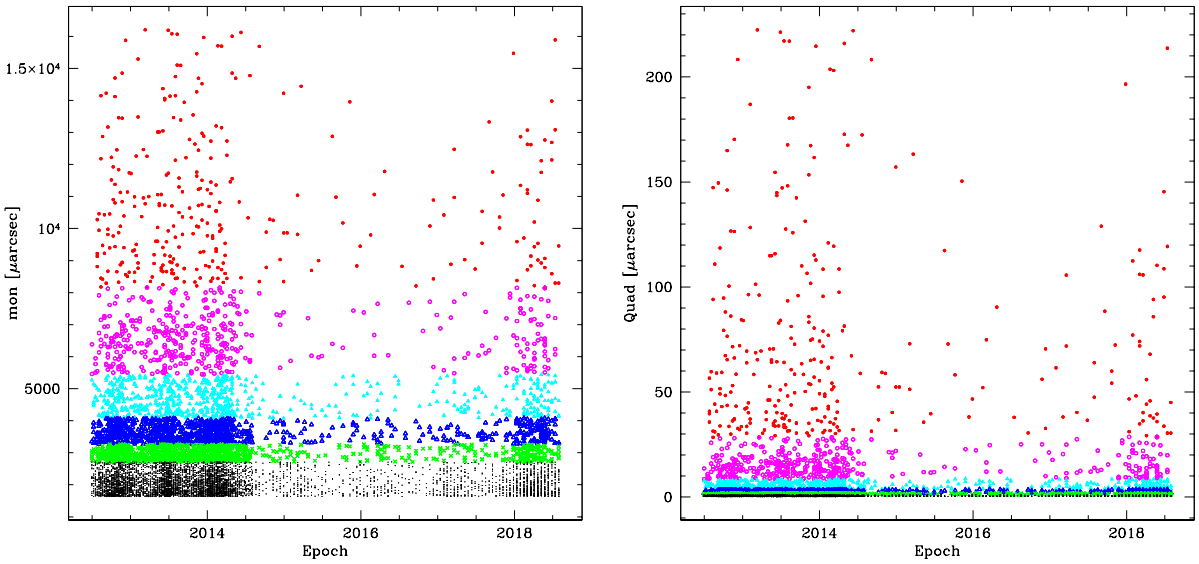

Figure 5. The monopole (left-hand side) and quadrupole (right-hand side) deflections over all epochs of Jupiter's visibility for all stars up the magnitude limit V=20, where $1 < b/R_J \leq 2$ (full square), $2 < b/R_J \leq 3$ (open square), $3 < b/R_J \leq 4$ (open triangle), $4 < b/R_J \leq 5$ (full triangle), $5 < b/R_J \leq 6$ (cross), $b/R_J > 6$ (dots).

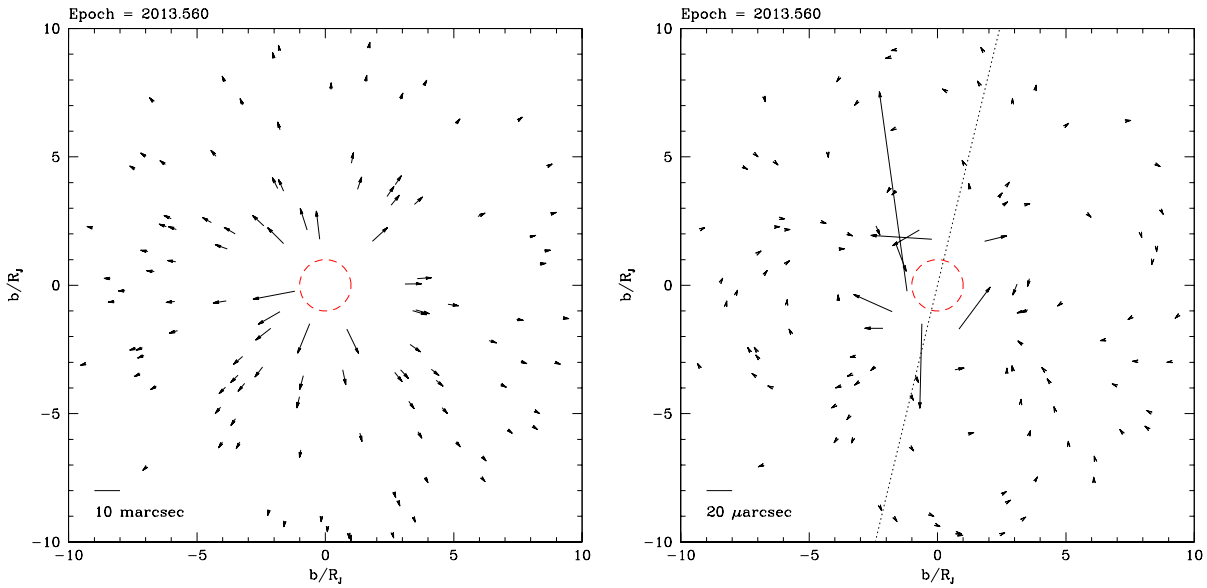

Figure 6. Observer view of the monopole (left-hand side) and quadrupole (right-hand side) light deflection vector field around Jupiter (circle) in mid 2013. The scales of 10 marcsecond for the monopole and 20 μarcsecond for the quadrupole are shown on the lower left of the plots, while the dotted line indicates the direction of the Jupiter's spin axis with respect to the line-of-sight.

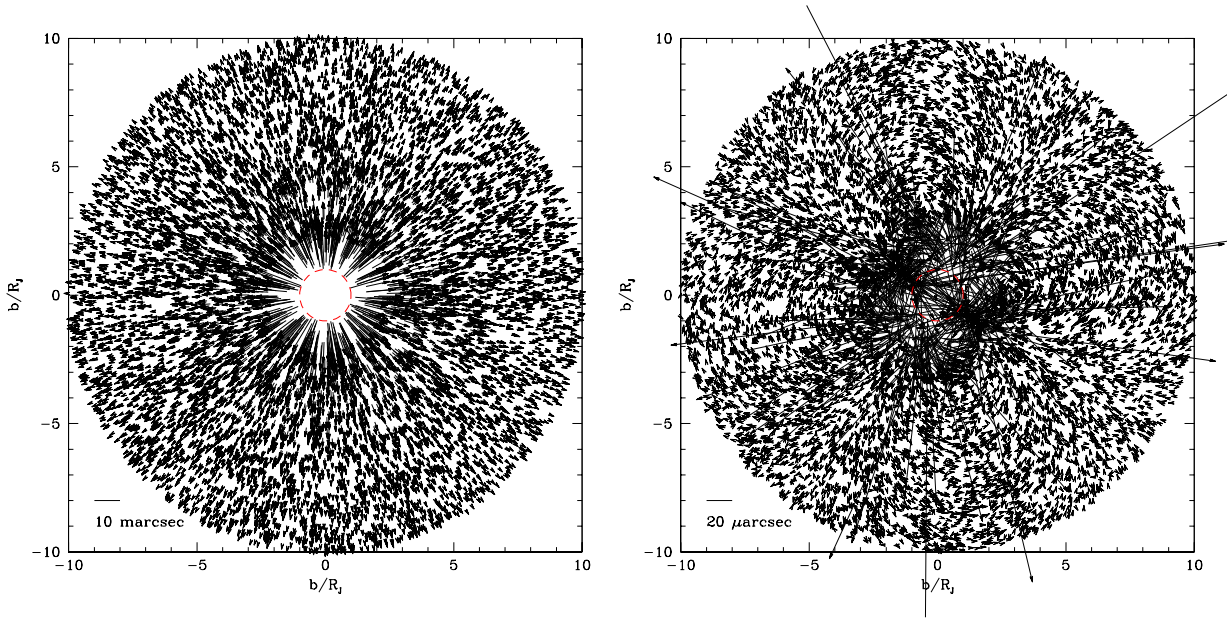

Figure 7. The monopole (left-hand side) and quadrupole (right-hand side) stellar vector field around Jupiter (circle) over the epochs between 2012 and 2018 from the observer point of view. The scales of 10 mas for the monopole and 20 μas for the quadrupole are shown on the lower left of the plots.

4. Measurement of the deflection

4.1. Processing the observations for γ and J_2

The observed quantities used to fit the relativistic effect in the light deflection are the along-scan positional differences of the stars referred to a common origin, namely the center of gravity of Jupiter. More precisely, we have estimated the measurements ($\Delta\mathbf{\Phi}_{als}$) along scan between two transits: the first one with Jupiter ($\mathbf{\Phi}_{+J}$) and the second one without Jupiter ($\mathbf{\Phi}_{-J}$), *i.e.*:

$$\Delta\mathbf{\Phi}_{als} = \mathbf{\Phi}_{+J} - \mathbf{\Phi}_{-J}. \tag{18}$$

As stated by (18), the method rests only on the comparison between small fields taken at two distinct epochs (each point on the sky will be mapped at least three times during six months) and it is largely independent from the attitude reconstruction of Gaia. This makes possible, in estimating the final accuracy, to consider only random errors and not the systematic attitude errors shared by all the sources at the two epochs.

The set of n observations can be considered as a system of n equations where the unknowns are the parameters γ and ϵ. The condition matrix is calculated by evaluating the partial derivatives with respect to γ and ϵ in (18). The large number of stellar measurements, about 160,000 for 90 Jupiter observations scattered over the 5-year mission is solved for the two unknowns with a weighted least squares procedure using singular value decomposition. The off-diagonal terms of the final covariance matrix are not significant, indicating a very weak correlation between the two fitted parameters.

Finally anomalous observations are filtered out with an iterative Student ratio test on the residuals.

The estimate of the accuracy with which Gaia could determine γ and ϵ from small field astrometry has been estimated by running more than 100 times this numerical simulation with random drawings stochastically independent in each experiment. The average of the 100 values of γ and ϵ prove that there is no bias in the determination as seen in figure 8. As for the precision, the scatter was taken as a more robust way to assess the accuracy than the formal error of the diagonal terms of the covariance matrix. The mean and scatter have been evaluated by using the usual point estimates valid for $n_{run} \gg 1$:

$$< \gamma > = \frac{1}{n_{run}} \sum_{i=1}^{n_{run}} \gamma(i) \tag{19}$$

$$< \epsilon > = \frac{1}{n_{run}} \sum_{i=1}^{n_{run}} \epsilon(i) \tag{20}$$

$$\sigma_\gamma = \sqrt{\frac{1}{n_{run}} \sum_{i=1}^{n_{run}} \gamma(i)^2 - < \gamma >^2} \tag{21}$$

$$\sigma_\epsilon = \sqrt{\frac{1}{n_{run}} \sum_{i=1}^{n_{run}} \epsilon(i)^2 - < \epsilon >^2}. \tag{22}$$

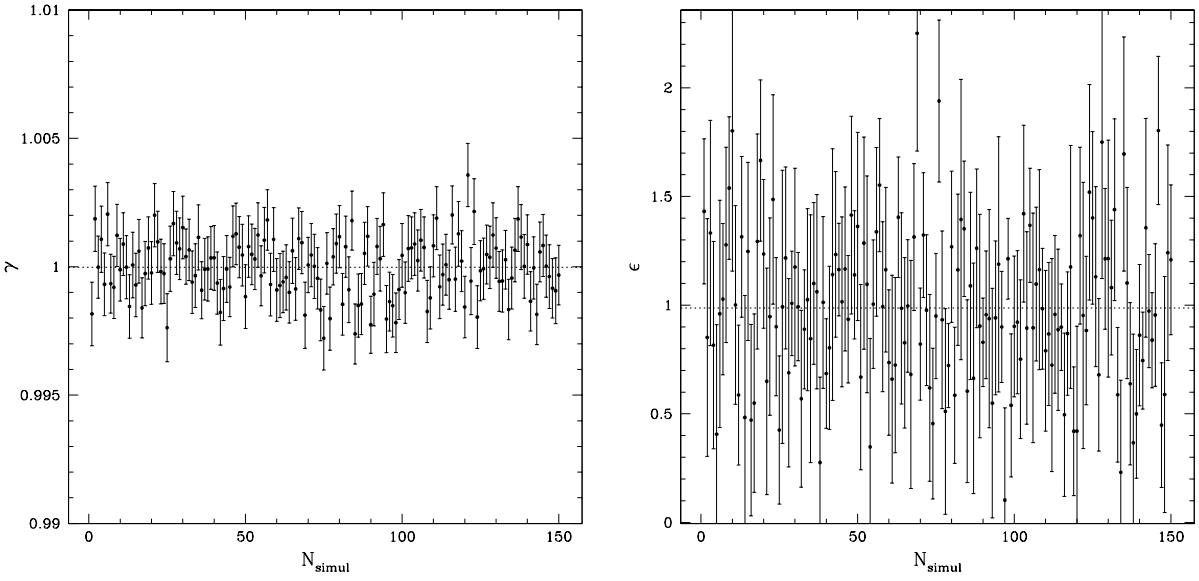

Figure 8. The distribution of the mean values of γ (left-hand side) and ϵ (right-hand side) over 150 Montecarlo simulations. The bars are the standard deviations.

4.2. Results

The main results are listed in table 3 with the average and scatter on γ and ϵ for three independent Montecarlo runs.

Table 3. Results for the mean value and scatter of γ and ϵ in Montecarlo experiments of different lengths.

$<\gamma>$	σ_γ	$<\epsilon>$	σ_ϵ	runs
0.9910	1.0295×10^{-3}	1.012	0.335	50
1.0000	1.1473×10^{-3}	0.992	0.358	100
1.0000	1.1456×10^{-3}	0.986	0.361	150

It is found with all the assumptions described in the previous sections that γ can be determined from the monopole light deflection by Jupiter with an uncertainty of 1.1×10^{-3}. This is three times better than the optical determination achieved by Hipparcos, the previous astrometric ESA mission, with stellar astrometry at large angles from the Sun [28] and 5 million observations of stars. The interest rests not only on the accuracy achieved (the global astrometry should reach four orders of magnitude better with solar light-bending), but on the fact that (i) it can be done with a planet, (ii) it is a prerequisite to the detection of the quadrupole effect in the residuals, (iii) it opens the way for testing the accurate modelling of the deflection by a moving body (it is stationary in our experiments).

The final result in ϵ confirms that the gravitational effect due to J_2 is detectable with Gaia (albeit marginally), with typically $\epsilon = 1 \pm 0.35$, that is to say a 3-σ detection. The effect of J_4 is negligible since it is much smaller than the random noise on most stars. Using $J_4 \sim -0.0006 \sim 4J_2/100$ this results for a grazing ray into a deflection of 10μas. In addition the effect of J_4 decreases as $(R_J/r)^5$ instead of $(R_J/r)^3$ and very few stars close to the planet limb would contribute to the signal.

4.3. Best strategy for the actual experiment

The above results concern a statistical analysis over all the epochs of observations during five years, it is however useful to see whether some controlled parameters are more favorable than others to observe the light bending effect and if one can restrict the risk of systematic errors. First of all we have considered the evolution of the errors on γ and ϵ with the limiting magnitude, for various impact parameters and for all the epochs. As we include fainter stars, they get more numerous but each with a smaller weight due to the degradation of the astrometric accuracy. It was not obvious what effect would overcome the other: could many faint stars contribute significantly or not?

The risk being to increase significantly the chance of systematic deviation for almost no improvement in the solution.

The results are plotted in figure 9, where the precision is shown when only stars brighter than V are used in the fit. Each curve corresponds to a limitation in the size of the field of view around Jupiter. It's clear (and not surprising) that using the full Gaia field provides the best results, in particular for γ just because the monopole deflection decreases more slowly with increasing impact parameter than the quadrupole's. However going further than $30R_J$ brings very marginal improvement and this can be used to determine what a small field experiment means in practice. Conversely below 10 R_J the number of stars decreases very quickly and at 5 R_J we usually have no star brighter than V=17.5. As for the magnitude it seems that one could also reject stars (in case of calibration problems for example) fainter than $V = 16$ without much loss as the final precision on γ and ϵ does not improve very much when they are included. That's a very nice feature when it comes the time to decide on whether faint stars are useful or not. The graphs show also a degradation in precision when only the brightest stars are considered, probably because the number of stars becomes too small to be significant and formula (17) inserts a constant error in this case. Then another interesting experiment

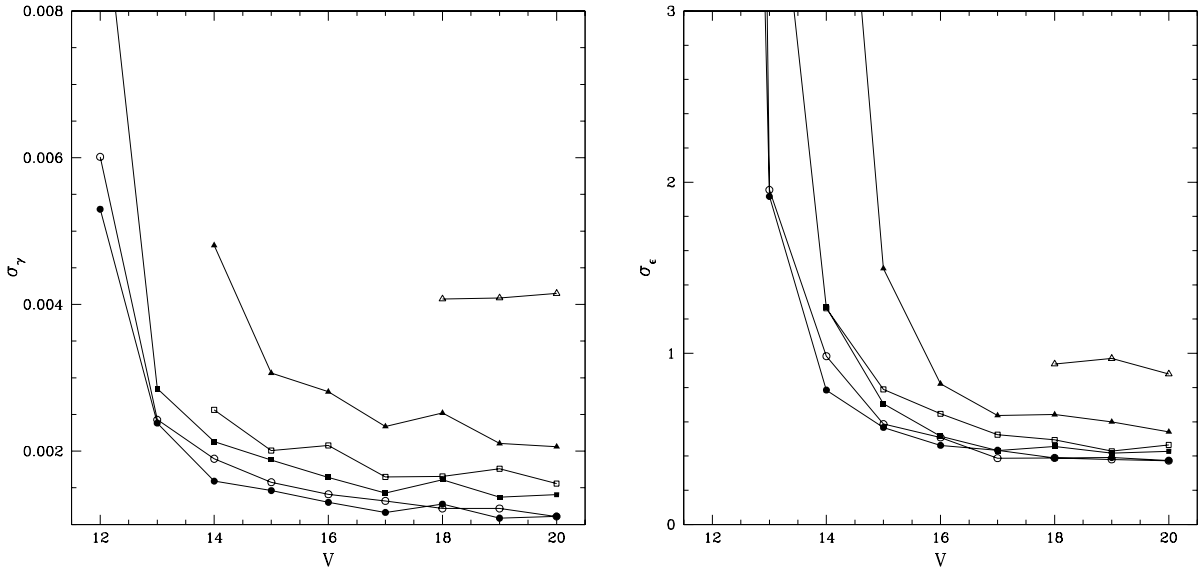

Figure 9. Evolution of the errors on γ and on ϵ with the magnitude and for various impact parameters. Full circles indicate the complete field corresponding to 45 R_J, open circles 30 R_J, full squares 20 R_J, open squares 15 R_J, full triangle 10 R_J and, open triangle 5 R_J.

has been run to test what would be the result if one selected only the few epochs during which we have the maximum number of stars in the background field, that is to say around 2013 when Jupiter is close to the Galactic plane. To this purpose, figure 10 shows again the evolution of the errors with magnitude, when all observations at every

epoch are included (full circles) or only during the crossing of the Galactic plane in 2013-2014 (open circles with only 20 epochs instead of 90 in the nominal experiment). Not surprisingly the errors are larger when considering only the best epochs, but not dramatically larger, showing that a strategy may be applied to perform valuable and dedicated experiments during the first two years of the mission, to validate the concept and get already significant results.

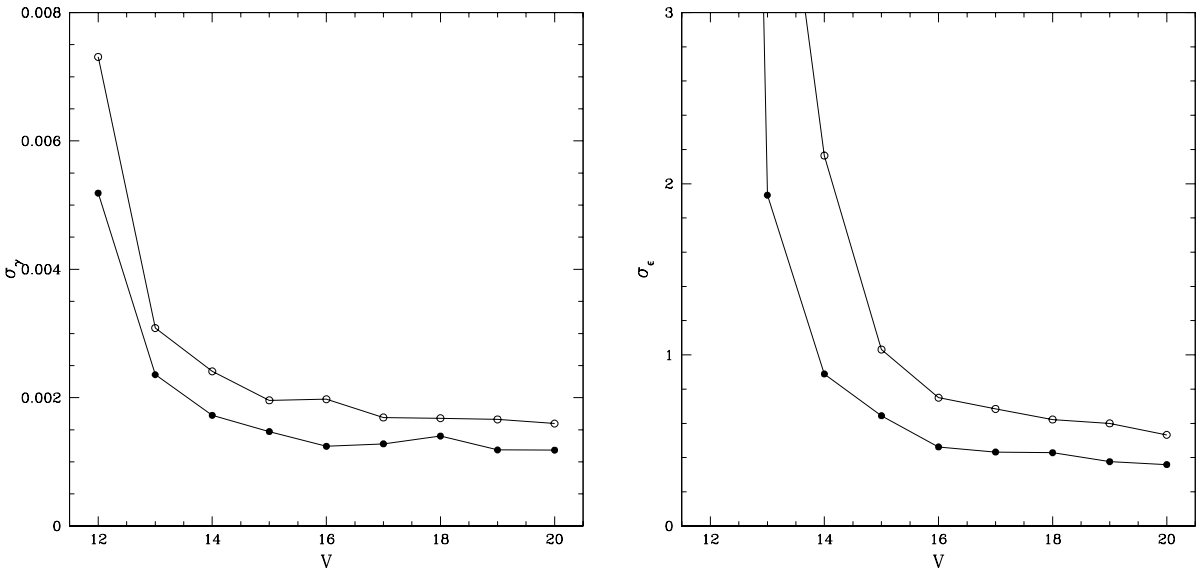

Figure 10. The evolution of the errors with magnitude, keeping the whole Gaia field for all epochs (full circles) and for 2013 (open circles), when we have the maximum number of stars.

Finally one should also look at the passage of Jupiter in the middle of a concentrated open cluster with stars brighter than $V = 13$. There are many such clusters on the ecliptic in the direction of the Sagittarius, that Jupiter will cross in 2019. This is after the nominal mission completion, but well within the possible extended mission permitted by the consumable. This kind of experiment would obviously add in the science case to support this extension of the operations. To this aim we have run the simulator with bright stars and a surface density comparable to that found in these open clusters. Results for the determination of γ and ϵ are given in table 4 and table 5 with all the stars of 12 or 13 magnitude respectively. Two realistic concentrations have been considered around Jupiter corresponding to fields of 3 and 6 arcmin around the planet. One sees that a single experiment can do almost as well as the 5-year mission, provided the number of bright stars in the cluster is large enough. Note that we have excluded a priori all the stars with magnitude range between 14 and 16, which statistically contribute significantly to the precision. At this point this is just an indication showing that a detail investigation on specific clusters is worth doing.

Table 4. Precisions computed after 150 Montecarlo runs selecting special fields in 2013 and increasing artificially the number of stars (n*) (V=12).

	n*	σ_γ	σ_ϵ
$b = 7R_J$			
	1	7.41×10^{-3}	14.54
	5	3.37×10^{-3}	2.73
	13	1.62×10^{-3}	0.69
	20	1.39×10^{-3}	0.34
	27	1.06×10^{-3}	0.32
	34	9.31×10^{-4}	0.27
$b = 15R_J$			
	7	4.48×10^{-3}	9.09
	23	2.12×10^{-3}	1.51
	39	1.70×10^{-3}	0.94
	63	1.31×10^{-3}	0.62
	79	1.26×10^{-3}	0.51
	119	9.16×10^{-4}	0.30

Table 5. Precisions computed after 150 Montecarlo runs selecting special fields in 2013 and increasing artificially the number of stars (n*) (V=13).

	n*	σ_γ	σ_ϵ
$b = 7R_J$			
	9	2.49×10^{-3}	1.51
	29	1.16×10^{-3}	0.37
	49	9.53×10^{-4}	0.26
	66	7.50×10^{-4}	0.20
	91	6.50×10^{-4}	0.15
$b = 15R_J$			
	44	1.88×10^{-3}	1.28
	67	1.56×10^{-3}	0.62
	81	1.43×10^{-3}	0.58
	97	1.17×10^{-3}	0.41
	127	1.09×10^{-3}	0.35

5. Conclusion

The objectives of this paper has been to study a new way to determine the PPN parameter γ by exploiting a method of differential positional measurements around Jupiter and to assess the detection of the light bending from the quadrupole moment of Jupiter. Thanks to the high astrometric accuracy to be achieved by the ESA astrometry mission Gaia and the repeated observations over five years this will be feasible as the new design of Gaia's optical instrument allows to process stellar observations very close to the surface of giant bodies. We have shown that the deviation to GR with the monopole deflection can be assessed to 10^{-3} with Jupiter only, a result in the visible better than the optical accuracy already achieved by Hipparcos with the stars and the solar light bending. With the same observations, the quadrupole light deflection will be detectable for the first time with a 3-σ confidence level.
Although we have designed an ideal and simplified experiment it includes realistic observations of Jupiter feasible with Gaia, taking into account the astrometric accuracy with the star's magnitude deduced from the current error budget analysis. Whereas the Gaia concept and its design rest entirely on the global astrometry we have given for the first time a realistic figure on the true strength of Gaia to carry out also relativity testing with small field astrometry and propose some strategies to carry out this experiment in the best conditions. When the initial conditions of the Gaia scanning law are known, the same principles will be applied using a real stellar distribution. The method will be also extended to the observations of Saturn, at least for the monopole effect.

Acknowledgments

MTC acknowledges financial support from the Henri Poincaré Fellowship during her stay at the Observatoire de la Côte d'Azur (Cassiopée Department). We wish to thank the members of the *Relativistic and Reference Frame Working Group* of Gaia for their valuable comments and collaboration.

Appendix A

This appendix shows the set of fundamental integrals computed to obtain expressions (11) and (12) for the deflection vector $\mathbf{\Delta\Phi}$ after having scaled the photon length by the impact parameter:

$$\int \frac{d\lambda}{(1+\lambda^2)^{3/2}} = \frac{\lambda}{(1+\lambda^2)^{1/2}}$$
$$\int \frac{d\lambda}{(1+\lambda^2)^{5/2}} = \frac{\lambda/3}{(1+\lambda^2)^{3/2}} + \frac{2\lambda/3}{(1+\lambda^2)^{1/2}}$$
$$\int \frac{d\lambda}{(1+\lambda^2)^{7/2}} = \frac{\lambda/5}{(1+\lambda^2)^{5/2}} + \frac{4\lambda/15}{(1+\lambda^2)^{3/2}} + \frac{8\lambda/15}{(1+\lambda^2)^{1/2}}$$
$$\int \frac{\lambda d\lambda}{(1+\lambda^2)^{5/2}} = -\frac{1/3}{(1+\lambda^2)^{3/2}}$$

$$\int \frac{\lambda d\lambda}{(1+\lambda^2)^{7/2}} = -\frac{1/5}{(1+\lambda^2)^{5/2}}$$
$$\int \frac{\lambda^2 d\lambda}{(1+\lambda^2)^{7/2}} = -\frac{\lambda/5}{(1+\lambda^2)^{5/2}} + \frac{\lambda/15}{(1+\lambda^2)^{3/2}} + \frac{2\lambda/15}{(1+\lambda^2)^{1/2}}$$

Appendix B

Let us consider the angle φ, ϑ of the Jupiter axis with respect the orthonormal directions $\mathbf{n}$, and $\mathbf{t}$, respectively. From the left hand-side of equation (13) we get

$$1 - 2(\mathbf{n}\cdot\mathbf{z})^2 - 2(\mathbf{t}\cdot\mathbf{z})^2 = -\sin^2\vartheta\cdot\cos 2\varphi, \tag{B.1}$$

and from that one of equation (14)

$$2(\mathbf{n}\cdot\mathbf{z})(\mathbf{m}\cdot\mathbf{z}) = \sin^2\vartheta\sin 2\varphi. \tag{B.2}$$

Then, the modulo of the quadrupole deflection term, let's say $\Delta\mathbf{\Phi}_{quad}$, in equation (10)) will depend only on $\sin^2\vartheta$, namely on the angle between the $\mathbf{z}$ axis of Jupiter and the direction from the star to the observer

$$|\Delta\mathbf{\Phi}_{quad}| = \frac{2(1+\gamma)MJ_2R^3}{b^3}\sin^2\vartheta \tag{B.3}$$

Clearly, when the $\mathbf{z}$ lies on the $\{\mathbf{n},\mathbf{m}\}$ plane, i.e. $\mathbf{z}$ perpendicular to the line-of-sight, the quadrupole term will give its maximum contribution.

For a star in direction α with respect to the orthonormal axis $\{\mathbf{m},\mathbf{n},\mathbf{t}\}$ the modulo has a fixed value depending only on the star's direction of arriving with respect to the above frame centered on Jupiter, namely:

$$|\Delta\Phi_{quad}\mathbf{n}| = \mid \Delta\mathbf{\Phi}_{quad} \mid \cos 2\alpha \tag{B.4}$$

$$|\Delta\Phi_{quad}\mathbf{m}| = \mid \Delta\mathbf{\Phi}_{quad} \mid \sin 2\alpha. \tag{B.5}$$

References

[1] 2005 *Proc. of the Symposium The Three-Dimensional Universe with Gaia (Paris)* **ESA-SP-576**
[2] Will C M 1993 *Theory and experiment in gravitational physics* (Cambridge University Press)
[3] Turyshev S G, Williams J G, Nordtvedt K Jr, Shao M and Murphy T W 2003 *Lect. Notes Phys.* **648** 301-320
[4] Damour T and Nordtvedt K 1993 *Phys. Rev. Lett.* **70** 2217
[5] Bertotti B, Iess L and Tortora P 2003 *Nature* **425** 374
[6] Gravity Probe B Project at Stanford University, http://einstein.stanford.edu/
[7] Mignard F 2002 *Gaia: A European Space Project* vol. 2 (EAS Publications Series) p 105
[8] Vecchiato A, Lattanzi M G, Bucciarelli B, Crosta M T, de Felice F and Gai M 2003 *A&A* **399** 337
[9] Turyshev S G, Shao M and Nordtvedt K L 2004 *J.Mod.Phys.* **D13** 2035-2064
[10] Fomalont E B and Kopeikin S M 2003 *Astrophys.J.* **598** 704-711
[11] Kopeikin S M and Mashhoon B 2002 *Phys. Rev.* D **65** 064025
[12] Carlip S 2004 *Class. Quantum Grav.* **21** 3803-3812
[13] Will C M 2003 *Astrophys.J.* **590** 683-690
[14] Asada H 2002 *Astrophys.J.Lett.* **574** L69
[15] Samuel S 2004 *Int. J. Mod. Phys.***D 13** 1753

[16] Frittelli S 2003 *MNRAS* **344** L85-L87
[17] Kopeikin S M 2004 *Class. Quantum Grav.* **21** 3251-3286
[18] Pascual-Sànchez J F 2004 *Int.J.Mod.Phys.* **D 13** 2345
[19] Klioner S 2003 *Astron.J.* **125** 1580
[20] de Felice F, Crosta M T, Vecchiato A, Lattanzi M G and Buciarelli B 2004 *Astrophys.J.* **607** 580
[21] Le Poncin-Lafitte C, Linet B and Teyssandier P 2004 *Class. Quantum Grav.* **21** 4463
[22] Kopeikin S M 1997 *J.Math.Phys.* **38** 2587
[23] Le Poncin-Lafitte C and Teyssandier P 2004 *Proc. of the Journées Systèmes de Référence Spatio-Temporels (Obs. Paris)* p 204-209
[24] Hestroffer D and Berthier J 2005 *Proc. of the Symposium The Three-Dimensional Universe with Gaia (Paris)* **ESA-SP-576** p 297-300
[25] Crosta M T and Mignard F 2005 *Proc. of the Symposium The Three-Dimensional Universe with Gaia (Paris)* **ESA-SP-576** p 281-284
[26] Misner C W, Thorne K S and Wheeler J A 1973 *Gravitation* (Freeman)
[27] Epstein R and Shapiro I 1980 *Phys. Rev.* D **22** 12
[28] Froeschlé M, Mignard F and Arenou F 1997 Proc. of the ESA Symposium Hipparcos - Venice 97 **ESA-SP-402** p 49-52